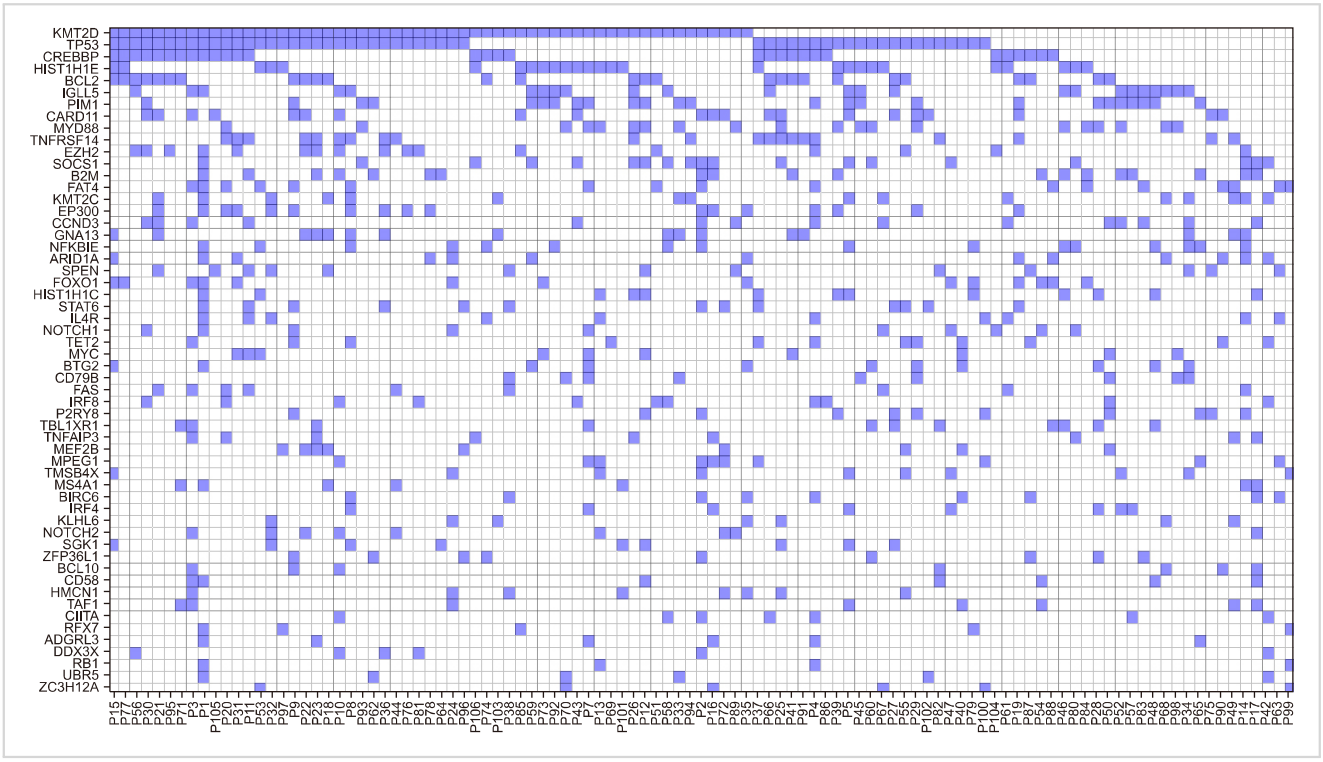

Supplementary Fig. 1. rrDLBCL patient driver alterations. A waterfall plot displays patients vs. alterations. Patients with at least 5 driver alterations from the Rushton *et al.* [9] analysis were included. Alterations affecting at least 5 patients were included. A total of 127 patients and 91 genes are included.

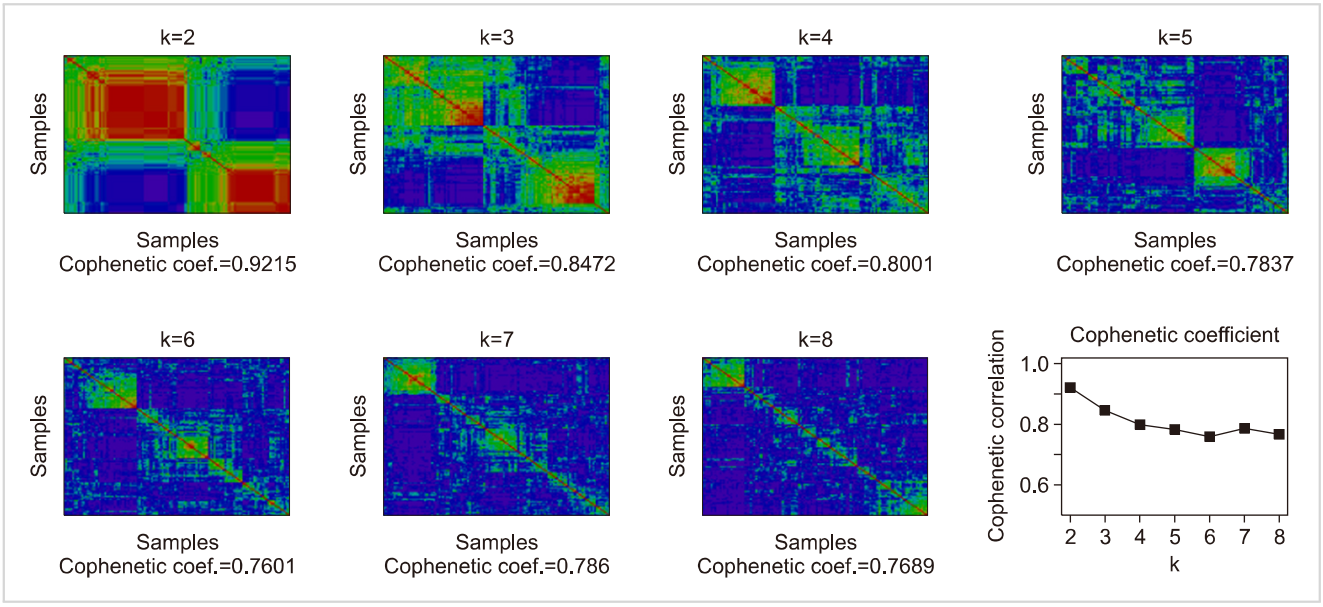

Supplementary Fig. 2. Comprehensive NMF clustering results. Analysis was directed examine between 2 and 8 clusters to fit the 127 rrDLBCL patients. NMF plots designate like-clustering cases in red, exclusionary cases in blue, and green as intermediate. The best-fit cophenetic value for all cases is documented by the dot plot on the bottom right.

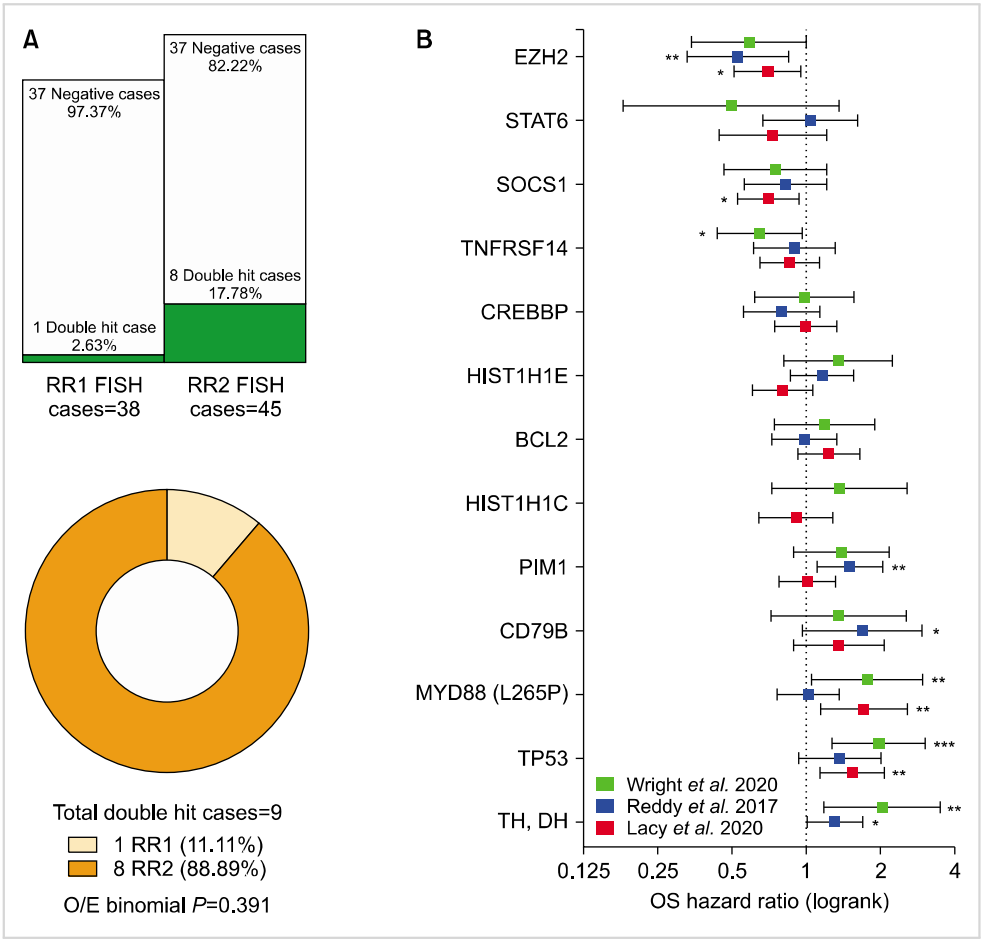

Supplementary Fig. 3. **(A)** Double Hit (DH) translocation cases are enriched in RR2. Patients with available translocation data are displayed in the bar graphs. Light grey (RR1) or dark grey (RR2) designates the presence of a DH case. The circle plot displays the distribution of DH cases across RR1 and RR2. 7 out of the 9 Double-Hit positive rrDLBCL cases also bore *TP53* alterations (77.8%) compared to negative cases (51.6%), another poor indicator of prognosis, but this proportion was not statistically significant (P=0.1711). Significance was measured for each comparison using an unpaired Welch's t-test. Bars represent the mean±SD. **(B)** Pretreatment hazard ratios of RR1 and RR2 genes exhibit differing favorable and unfavorable prognostic profiles. Three pre-treatment DLBCL cohorts were analyzed with Kaplan-Meier survival curves to measure the impact of each RR alteration on overall survival when treated with RCHOP. Significance was measured with Logrank analysis. The 95% confidence interval for each alteration is designated by error bars.

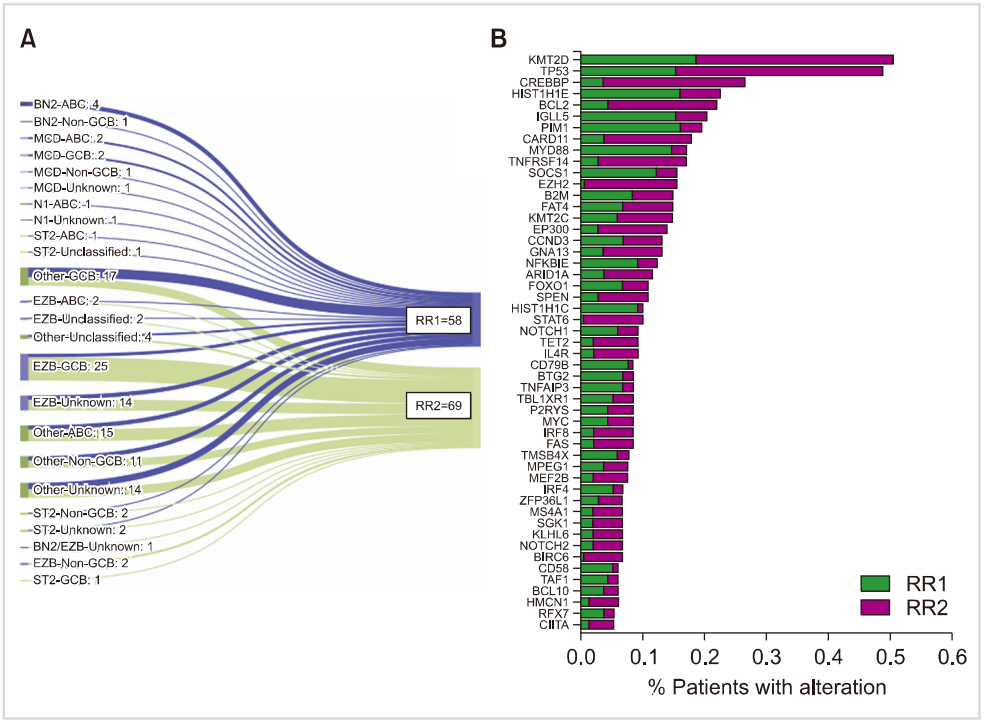

Supplementary Fig. 4. RR1 and RR2 composition based on DNA classification and COO classification. **(A)** A Sankey plot displays the composition of RR1 (blue) and RR2 (green) based on LymphGen alongside COO classification, as designated in Rushton *et al.* [9] **(B)** DNA alteration enrichment between RR1 and RR2 clusters. Proportion presence in RR1 (light grey) and RR2 (dark grey) families are displayed as stacked data that displays the total percentage present in the full Rushton *et al.* [9] population.

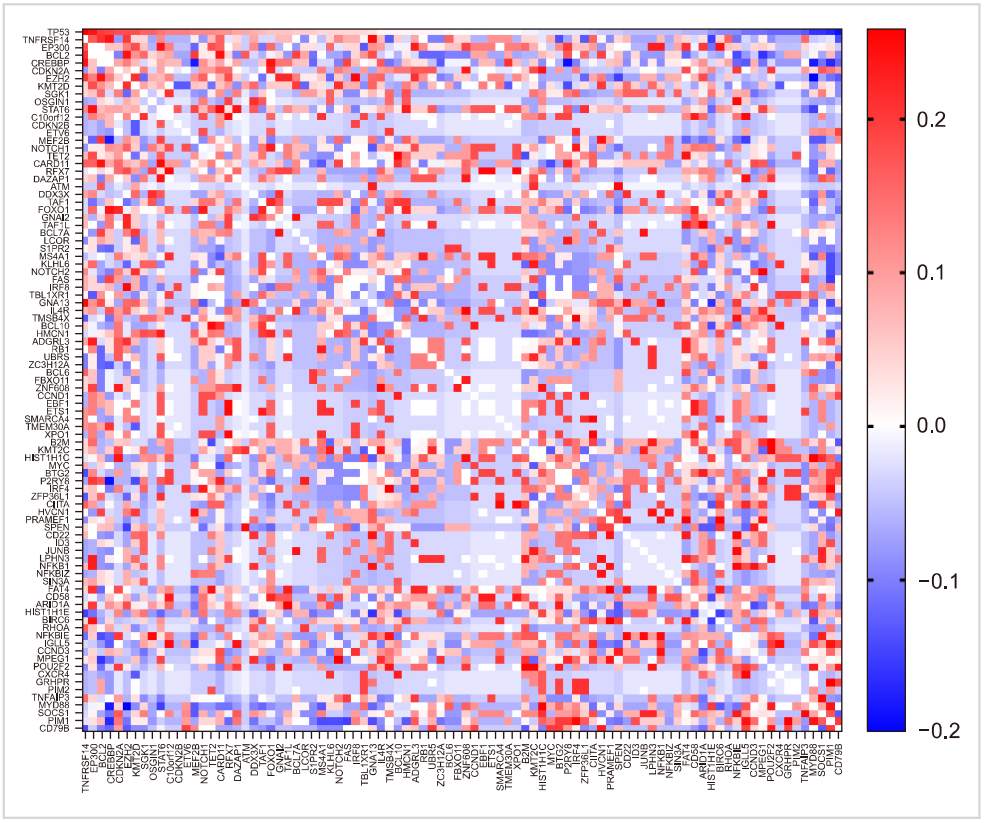

Supplementary Fig. 5. Pearson similarity matrix of all rrDLBCL gene alterations. Data is aligned to *TP53* alterations. Stronger co-association is designated by red and scaled down to blue for strong disassociation. Data were generated using GenePattern tools.

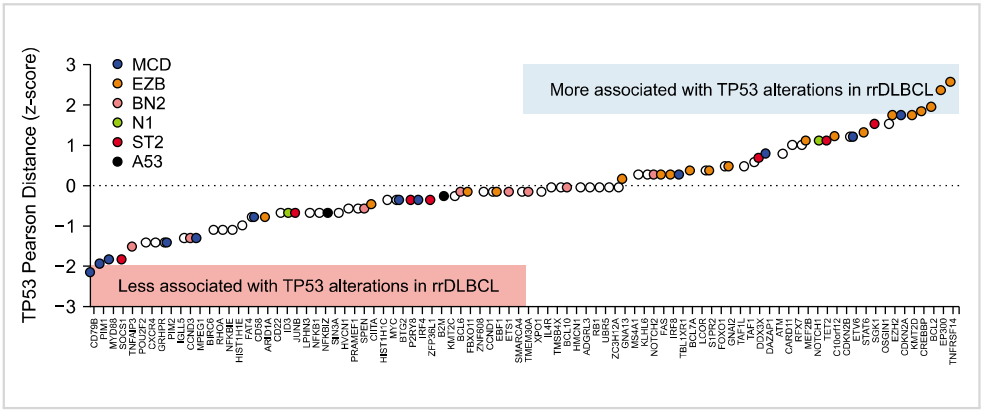

Supplementary Fig. 6. Pearson Distance from *TP53* alterations in rrDLBCL. Genes arranged from lowest to highest co-association with *TP53* alterations within the Rushton *et al.* [9] rrDLBCL cohort. Genes are designated by their associated LymphGen classification color.

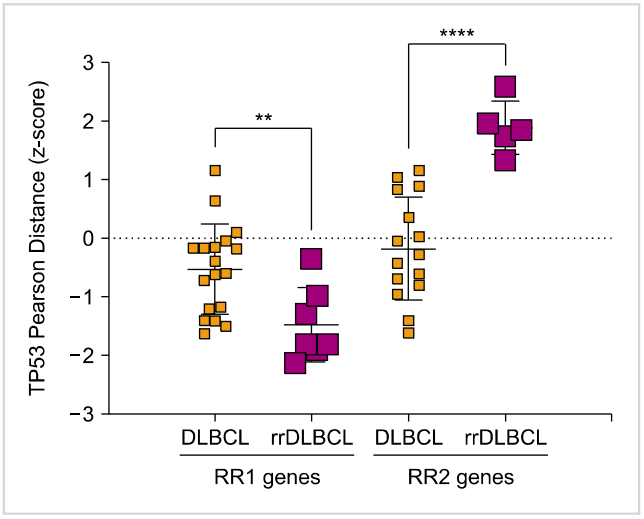

Supplementary Fig. 7. *TP53* alterations showcase significantly greater association with RR2 genes and significantly lower association with RR1 genes after rrDLBCL transition. Collective pretreatment Z-score normalized Pearson Distance values are presented for RR1 and RR2 subclassification genes before (3 cohorts) and after (1 cohort) transition to rrDLBCL. RR1 genes were significantly less associated with *TP53* ($P=0.0076$) and RR2 genes were significantly more associated with *TP53* alterations after relapse or refractory disease ($P<0.0001$).

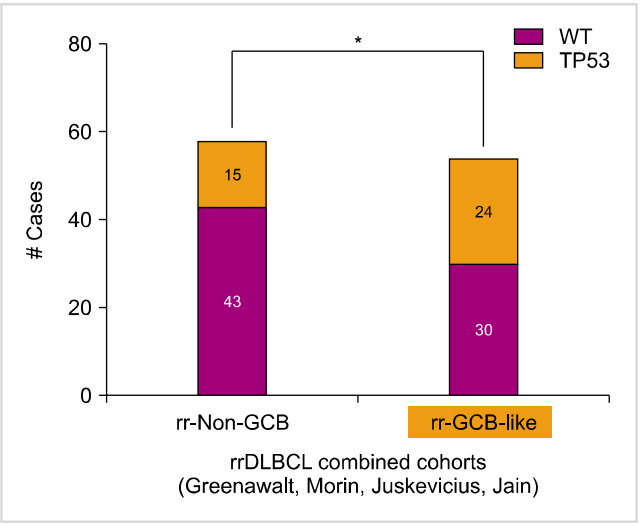

Supplementary Fig. 8. *TP53* alterations are significantly enriched towards GCB-like tumors in a collection of rrDLBCL cohorts. Bar graphs denote the presence of *TP53* alterations within GCB-like and non-GCB tumors. Significance was determined with a Fisher's Exact test.